Journal of Environmental Chemical Engineering 8 (2020) 104546

Contents lists available at ScienceDirect

Journal of Environmental Chemical Engineering

journal homepage: www.elsevier.com/locate/jece

An eco-friendly and low-cost strategy for groundwater defluorination: Adsorption of fluoride onto calcinated sludge

Renata S. Pigatto [a], Dison S.P. Franco [a], Matias S. Netto [a], Élvis Carissimi [b], Luis F.S. Oliveira [c], Sérgio L. Jahn [a], Guilherme L. Dotto [a,*]

[a] Chemical Engineering Department, Federal University of Santa Maria - UFSM, Santa Maria, RS, Brazil
[b] Department of Sanitation and Environmental Engineering, Federal University of Santa Maria - UFSM, Santa Maria, Brazil
[c] Universidad de la Costa, Department of Civil and Environmental Engineering, Barranquilla, Colombia

ARTICLE INFO

Editor: Despo Kassinos

Keywords:
Adsorption
Defluorination
Water treatment
World Health Organization

ABSTRACT

The excess of fluoride ions (F^-) in water for human supply is a serious public health. The recommended concentration of F^- ions by the World Health Organization (WHO) is 1.5 mg L^{-1}. Several groundwater sources around the world contain high F^- concentrations, and require treatment before human consumption. It was developed an eco-friendly and low-cost strategy for groundwater defluorination, i.e., adsorption onto calcinated sludge. This strategy was efficient at pH of 5.5 and using 5 g L^{-1} of calcinated sludge. The groundwater attained the WHO standard within 60 min. The kinetic model of pseudo-second-order obtained a better adjustment to the experimental data. The equilibrium curve at 25 °C was better represented by the Tóth model. The maximum adsorption capacity was 2.04 mg g^{-1}. Therefore, adsorption using calcinated sludge can be considered as an eco-friendly and low-cost strategy for groundwater defluorination.

1. Introduction

The water demand is increasing worldwide, and it is necessary to provide a suitable treatment to adequate it from distinct sources into potable regulation standards. From conventional treatment, great quantities of sludge are generated as solid waste, whose disposal must be adequate due to the use of iron- and aluminum-based metallic coagulants during the coagulation-flocculation stage [1,2]. In general, its composition is an amount rich in organic matter added to inorganic compounds, depending on factors as spring of raw water catchment and the applied treatment [2]. In the case of sludge containing trivalent aluminum ions, it is not possible to dispose of them on the soil or water bodies [3]. Such ions, however, confer a considerable surface area and potential for use as an adsorbent for several objectives [4].

Another serious problem is the contamination of the surface and groundwaters by the excess of fluoride ions. People exposed to the intake of such waters for a long period can suffer from fluorosis, a dental type of disease in the first stage, and skeletal when in an advanced stage [5]. The source of contamination in such water bodies can be both natural and anthropogenic, occurring in many places around the world [6]. The World Health Organization's recommendation for the maximum concentration of fluoride ions is of 1.5 mg L^{-1}, which is enough to fight the dental cavity [7]. On the contrary, water treatment must be proceeded to guarantee its potability.

There are different techniques for water defluorination, being them precipitation/coagulation, ion exchange, membrane separation, electrochemical treatment, and adsorption [6,8–10]. Among those, adsorption stands out under environmental and economic aspects besides its simple design and operation with good removal rates [8]. Thus, it is viable to apply this technique in remote regions supplied mainly by groundwater [11]. The most used adsorbent material is activated alumina, in line with the recommendations from the United States Environmental Protection Agency, with a good capacity of removal and regeneration, but with relatively high costs [12]. Other materials used are activated charcoal, bone char, mineral rocks, biosorbents, or residues, which present low costs and high local availability, as is the case of sludge [13].

In this work, it was investigated the potential of a calcinated sludge for groundwater defluorination. Sludge, which is a waste of great abundance and at no cost generated in conventional water treatment

* Corresponding author at: UFSM, 1000, Roraima Avenue, 97105-900, Santa Maria, RS, Brazil.
E-mail addresses: renata.pigatto@hotmail.com (R.S. Pigatto), francodison@gmail.com (D.S.P. Franco), matias_s_netto@hotmail.com (M.S. Netto), ecarissimi@gmail.com (É. Carissimi), lsilva8@cuc.edu.co (L.F.S. Oliveira), sergiojahn@gmail.com (S.L. Jahn), guilherme.dotto@ufsm.br (G.L. Dotto).

https://doi.org/10.1016/j.jece.2020.104546
Received 6 July 2020; Received in revised form 24 August 2020; Accepted 21 September 2020
Available online 28 September 2020

Table 1
Groundwater characteristics.

Property	Values
Fluoride	3.0 to 5.0 mg L^{-1}
Chloride	150 to 250 mg L^{-1}
Bromide	0 to 5 mg L^{-1}
Nitrate	0 to 1 mg L^{-1}
Sulfate	350 to 500 mg L^{-1}
pH	8.3 to 8.8
Conductivity	1600 to 1700 μS cm^{-1}

Table 2
Variables and levels used in CCRD for the optimization of defluorination.

Variables	Levels				
	−1.41	−1	0	1	1.41
Adsorbent dosage (g L^{-1})	1	1.58	3	4.42	5
pH	4	4.9	7	9.1	10

plants, comes specifically from the coagulation-flocculation step, which through its structural characteristics, such as chemical composition, can be used as an adsorbent for removing fluoride ions from both synthetic solutions and groundwater. The sludge was from a local water treatment plant (Santa Maria, RS, Brazil). The material was calcinated and carefully characterized. It was sampled groundwater from Faxinal do Soturno (RS, Southern Brazil) and synthetic solution of sodium fluoride for comparison purposes. The treatment was optimized by response surface methodology (RSM). Once the best conditions were obtained, kinetic and equilibrium studies were carried out. Thus, a treatment for the important public health problem, which is the excess of fluoride ions, capable of reducing the concentration under 1.5 mg L^{-1}, was proposed, through the reuse of a residue continuously generated in great amounts in conventional water treatment plants.

2. Material and methods

2.1. Obtainment, treatment, and characterization of the sludge

Raw sludge was collected from a water treatment plant (Rio Grande do Sul sanitation company, CORSAN) located in Santa Maria, RS, Brazil. The material was oven-dried at 80 °C for 24 h. Then, 50 g of the material was calcinated in an oven (device F3000, EDG brand) at 200 °C for 2 h with a heating rate of 10 °C min^{-1}, in an oxidizing atmosphere. The sludge was then washed with 1 L of a 20 % (v/v) alcohol/aqueous solution under magnetic stirring for 1 h. The solid material was separated by filtration and oven-dried at 80 °C for 24 h. The chemical species were acquired from Neon (Brazil) with analytical grade.

Calcinated sludge was characterized through X-ray diffraction (XRD), Fourier-transform infrared spectroscopy (FT-IR), scanning electron microscopy (SEM), energy dispersive spectroscopy (EDS), surface area analyses (BET) [14,15], point of zero charge (PZC) [16], and thermogravimetric analysis (TGA). Detailed procedures about these characterization techniques are presented in the supplementary material (*S.1.*).

2.2. Groundwater and fluoride solutions

The groundwater employed in this work was collected in Faxinal do Soturno, RS, Brazil. The groundwater characteristics are presented in Table 1. The variation of these characteristics is due to the temperature and seasons. Four samples were taken every two months from August 2018 to June 2019. For comparison with groundwater, synthetic fluoride solutions were also used in the defluorination experiments. These solutions were prepared with deionized water and sodium fluoride

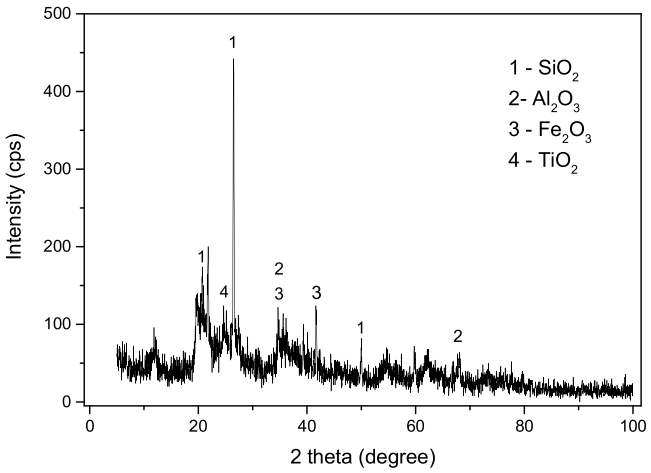

Fig. 1. XRD pattern of calcinated sludge.

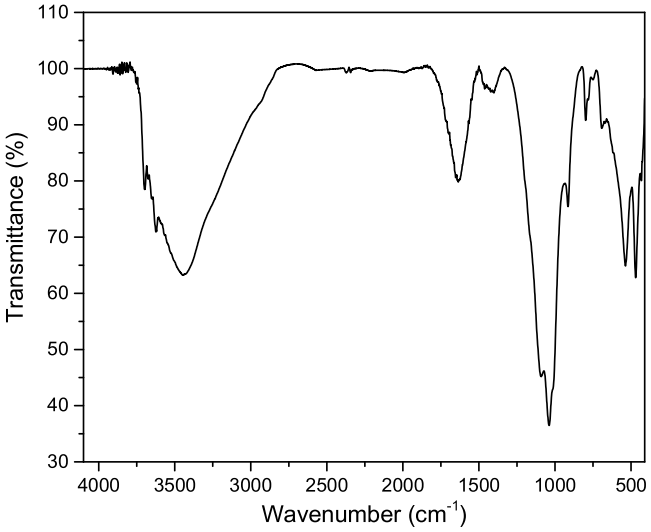

Fig. 2. FT-IR spectrum of calcinated sludge.

(Analytical grade, Belga Química, Brazil). A stock solution of 100 mg L^{-1} was prepared and diluted to obtain the concentrations of interest.

The fluoride concentrations were determined through ion chromatography (model: 930 Compact IC Flex, Metrohm, Swiss), with conductivity detector, chemical suppression, and CO_2 suppression. The compound separation was performed by an ionic change column (Metrosep A sup 5-150/4.0, Metrohm, Swiss) and pre-column (Metrosep A sup 5 Guard, Metrohm, Swiss) both with quaternary ammonium groups supported on polyvinyl alcohol, and accuracy of μg L^{-1}. The sample was pumped with a flow rate of 0.7 mL min^{-1} at a temperature of 30 °C. The eluent concentration presented the following composition: 3.2 mmol L^{-1} of sodium carbonate (Na_2CO_3, 99.95 % purity, Sigma Aldrich, USA), 1.0 mmol L^{-1} of sodium bicarbonate ($NaHCO_3$, 99.8 % purity, Sigma Aldrich, USA) and 20 % of acetone (CH_3COCH_3 UV/HPLC grade, Sigma Aldrich, USA). Sulfuric acid was employed as a chemical suppressor (H_2SO_4, 96.0 % purity, Sigma Aldrich, USA). The anion standard was prepared from a multi anions solution (bromide, chloride, nitrate, sulfate, fluoride and phosphate, SpecSol, Brazil).

2.3. Defluorination experiments

Defluorination experiments were carried in three steps: optimization experiments, kinetic experiments, and equilibrium experiments. All these experiments were carried out with plastic Erlenmeyers containing

100 mL of solutions, which were immersed in a Dubnoff type orbital shaker (MA095, Marconi) under the agitation of 150 rpm and 25 °C. For comparison, all the tests were performed with groundwater and also with synthetic fluoride solutions. After all experiments, samples were centrifuged, and the liquid was used for quantification.

In the optimization experiments, solutions were stirred for 2 h. The adsorbent dosage ranged from 1 to 5 g L^{-1}, and the pH ranged from 4 to 10. For the groundwater, the initial concentration of fluoride ions was 4.31 mg L^{-1}, and for the tests with the synthetic solutions, the initial concentration was 5.37 mg L^{-1}. In the kinetic experiments, curves were constructed with groundwater (initial F- concentration of 3.60 mg L^{-1}) and synthetic solutions (initial F- concentration of 5.37 mg L^{-1}). The curves were obtained in different pH values, i.e., 8.83 (natural pH) and 5.5. The adsorbent dosage was 5 g L^{-1}, and aliquots were withdrawn at 2.5, 5, 7.5, 10, 15, 20, 30, 60, 120, 240, and 300 min. For the isotherm experiments, curves were obtained with pH and initial F- concentration for groundwater and synthetic solutions equal to the kinetic tests. The adsorbent dosage varied from 1 to 15 g L^{-1}, and the solutions were stirred until the equilibrium.

2.4. Optimization of the defluorination process

Defluorination of groundwater and synthetic solutions using calcined sludge was optimized according to the adsorbent dosage and pH. The pH and dosage are operational conditions that influence the adsorption process/defluorination. The pH of the medium controls the magnitude of the electrostatic charges that are transmitted by the ionized adsorbate molecules, thus directly affecting the number of molecules that can be adsorbed. Also, the relation between the point of the zero charge (pH_{pzc}) and the pH can further increase the removal of fluoride. Concerning the dosage, the effects are related to the number of available sites per gram of material. In other words, the increase of the dosage causes an increase in the percentage of removal. However, higher dosages lead to lower adsorption capacity. Thus, aiming the optimization of these two independent variables, a Central Composite Rotational Design (CCRD) was used, this design considers 2 independent variables (k), and coded levels of -α, -1, 0, + 1, +α and axial spacing of 1.41 (2k/4). The levels and variables of CCRD are depicted in Table 2. The considered responses were fluoride removal percentage (*R*, %) and adsorption capacity (q_e, mg g^{-1}). The results were analyzed with the aid of the software *Statistica 8.0* (StatSoft, USA), proceeding to the analysis of variance (ANOVA) and the verification of the determination coefficient (R^2) and Fischer test to evaluate the variance and prediction of the model [17].

2.5. Kinetic and equilibrium of defluorination

The kinetic data describing the adsorption capacity of the calcinated sludge for fluoride (q_t, mg g^{-1}) over time *t* (min) were adjusted with several reaction models presented in the literature [18–21]. The models

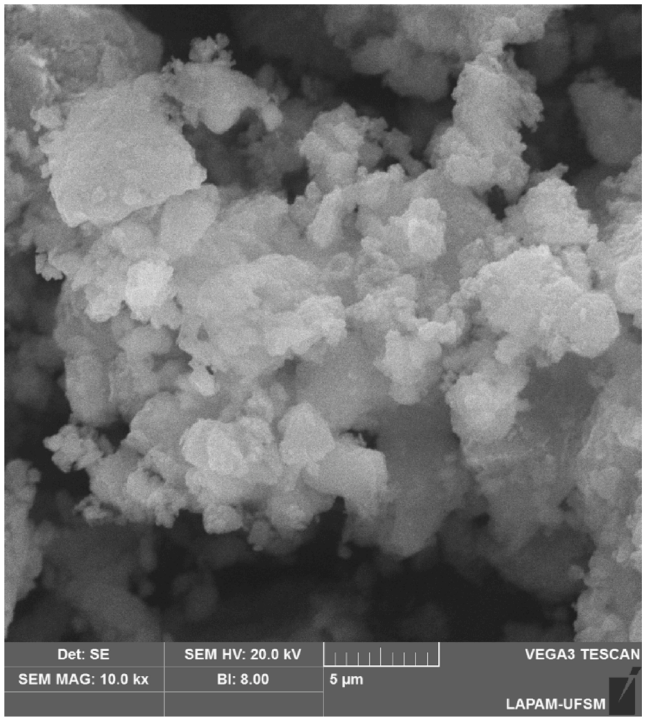

Fig. 3. Scanning electron microscopy of calcinated sludge.

Table 3
Semi-quantitative composition of the calcinated sludge.

Elements	Weight*	Atomic*
C (%)	23.39	31.57
O (%)	57.20	57.95
Mg (%)	0.17	0.11
Al (%)	7.86	4.72
Si (%)	8.01	4.63
K (%)	0.25	0.10
Ti (%)	0.22	0.07
Fe (%)	2.89	0.84

* determined by EDS.

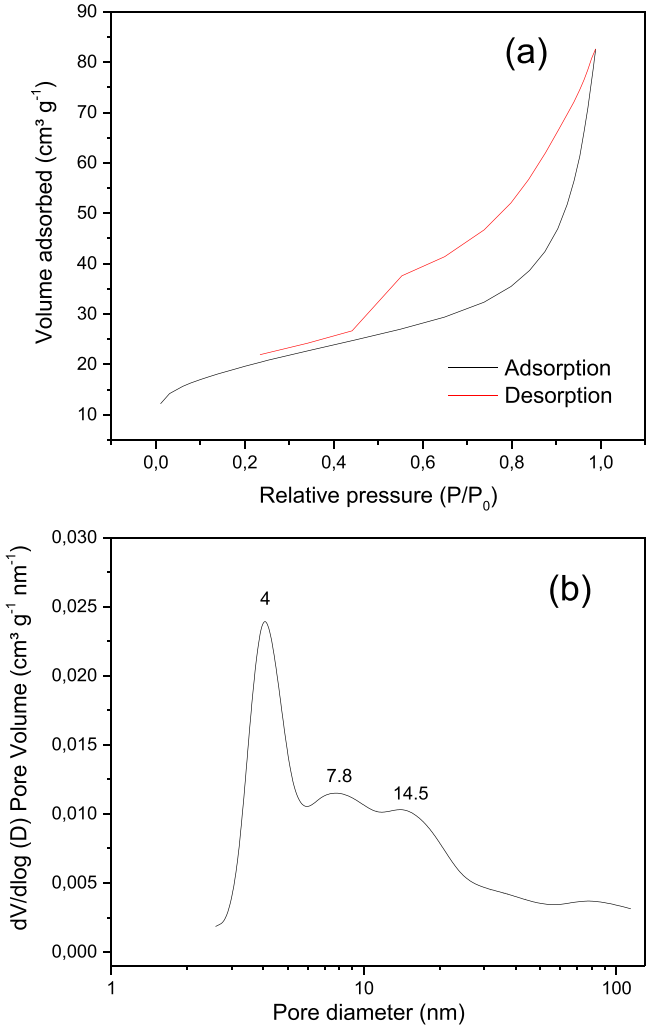

Fig. 4. (a) N_2 adsorption/desorption isotherms and (b) pore size distribution of calcinated sludge.

and its respective details are presented in the supplementary file (*S.2.*) The equilibrium data describing the adsorption capacity of the calcinated sludge for fluoride (q_e, mg g^{-1}) versus the remaining fluoride concentration in the solution (C_e, mg L^{-1}) were fitted with some isotherm models presented in the literature [22–25]. The models and their respective details are presented in the supplementary file (*S.3.*). The fit quality of the kinetic and isotherm models was evaluated by the determination coefficient (R^2), adjusted determination coefficient (R^2_{adj}), average relative error (*ARE*), and minimum squared error (*MSE*) (Supplementary file, *S.4.*).

3. Results and discussion

3.1. Calcined sludge characteristics

Fig. 1 shows the XRD spectra of the calcinated sludge used as a fluoride ion adsorbent. The sludge possesses a semi-crystalline structure, with a predominance of amorphous regions, according to the wide reflection range from 18 to 40°. The sludge has a complex chemical composition, containing predominantly oxides of silicon aluminum and iron, a structural characteristic that is shown in the diverse peaks found in the XRD. The peak at 20.73° and 26.5° indicates the presence of quartz in the calcined sludge [26,27]. The peak at 24.75° may be due to the presence of TiO_2 [28]. The peak at 37° may be due to the presence of Al_2O_3 and Fe_2O_3 in the calcined sludge [28]. The peak at 41.67° can be attributed to the presence of iron oxide in the calcined sludge [29]. The 50° peak can be attributed to the presence of quartz in the sample [30]. The peak at 68° may be due to the presence of Al_2O_3 in the calcined sludge [31].

The Fourier transform infrared spectrum of the calcinated sludge (Fig. 2) presents characteristic bands of materials of the same nature as the 3400−3700 cm^{-1} band associated with the stretching of the OH bonds [32]. The remaining organic matter presents several characteristic bonds in the range of 1050−1725 cm^{-1}, which may be C═C aromatic and C═O carbonyl conjugated in 1635-1643 cm^{-1} [33], vibrations due to the H—O—H bond between 1650−1600 cm^{-1} [32], OH deformation, symmetric COO— stretching and C—O stretching of phenolic groups in 1400−1465 cm^{-1} [34]. The Si—O bond is found at

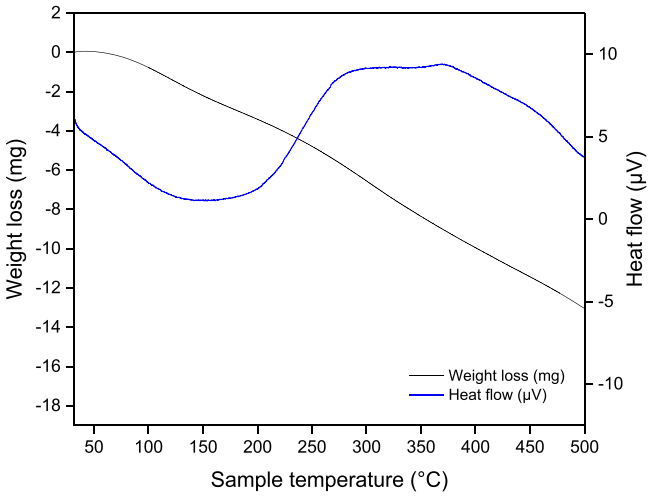

Fig. 5. TGA curves for calcinated sludge.

Table 4
Levels, factors, and responses for the CCRD used for fluoride adsorption.

pH	Adsorbent Dosage	Groundwater		Synthetic fluoride solution	
		R (%)	q_e (mg g^{-1})	*R* (%)	q_e (mg g^{-1})
−1	−1	67.52	1.84	60.89	2.07
1	−1	23.43	0.64	40.41	1.37
−1	1	86.08	0.84	85.10	1.03
1	1	42.00	0.41	66.48	0.81
−1.41	0	81.44	1.17	77.47	1.39
1.41	0	25.75	0.37	36.69	0.66
0	−1.41	14.15	0.61	33.33	1.79
0	1.41	60.56	0.52	86.96	0.93
0	0	51.28	0.74	74.49	1.33
0	0	48.96	0.70	73.93	1.32
0	0	50.12	0.72	74.12	1.33

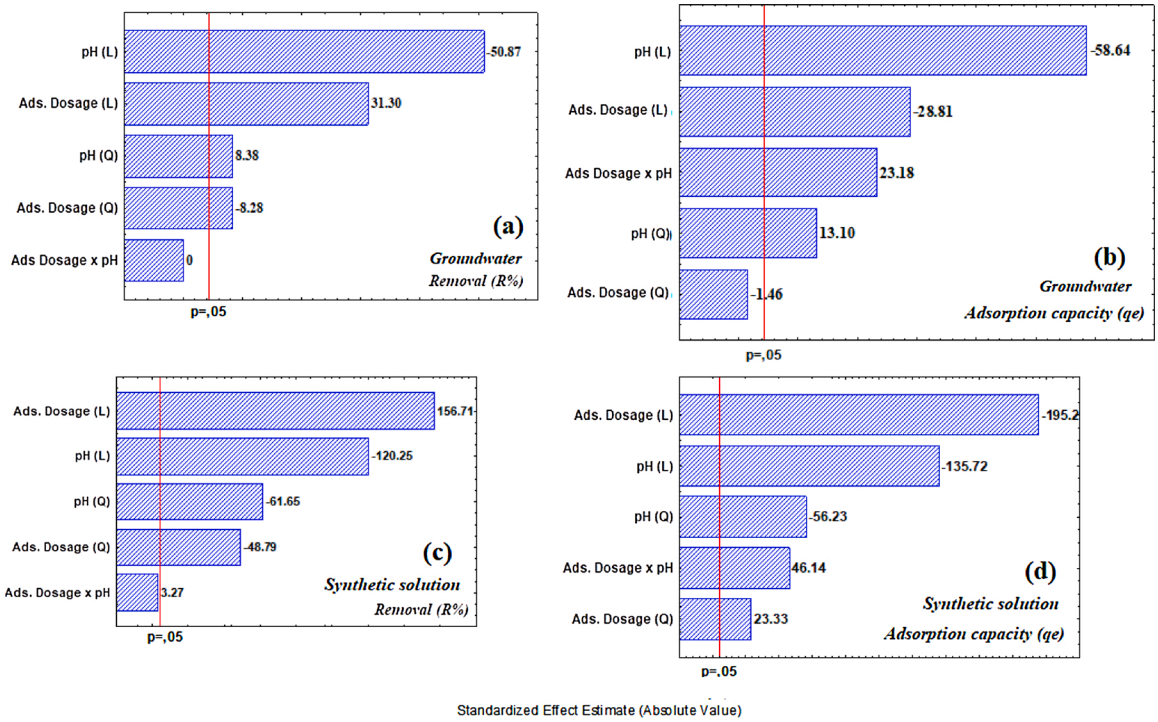

Fig. 6. Pareto graphs for the responses fluoride removal percentage (*R*) and adsorption capacity (q_e) in groundwater (a, b) and synthetic solutions (c, d).

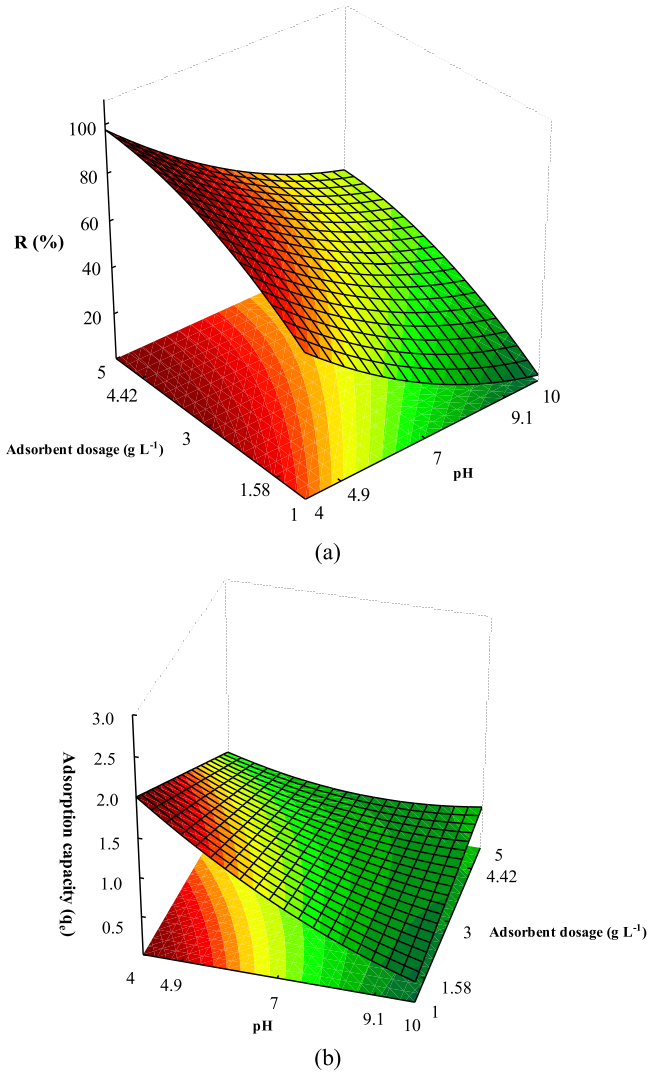

Fig. 7. Response surface curves for fluoride adsorption from groundwater: (a) R and (b) q_e.

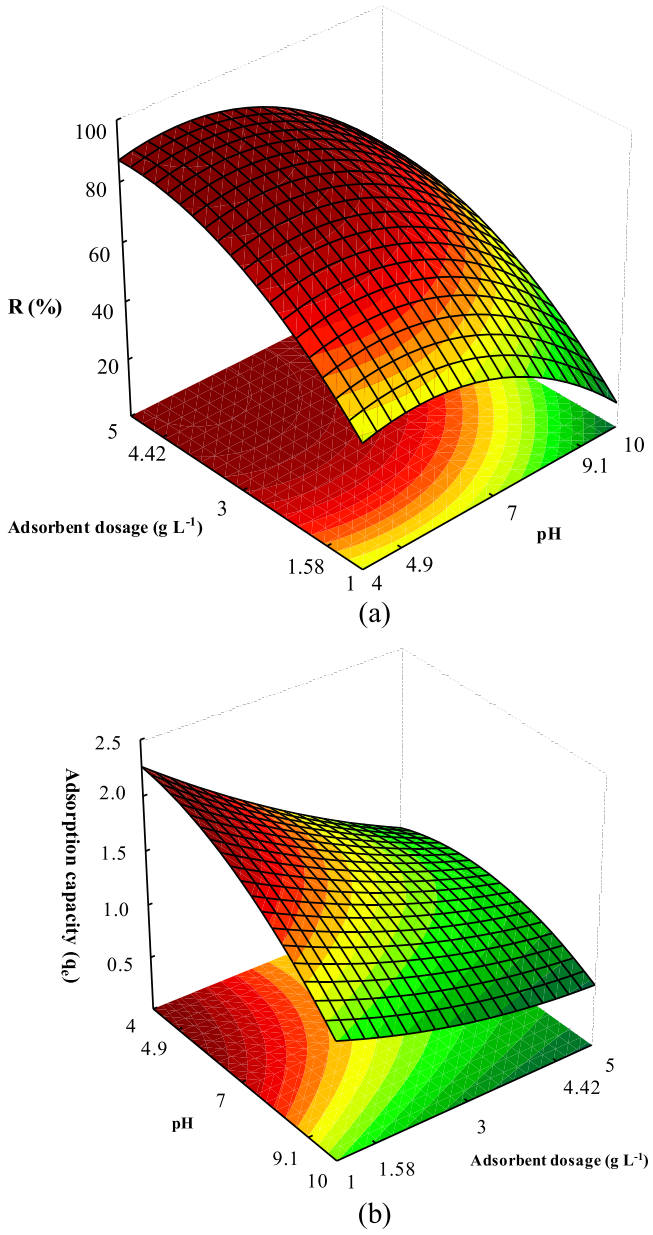

Fig. 8. Response surface curves for fluoride adsorption from synthetic solutions: (a) R and (b) q_e.

1035–1090 cm^{-1}, and the band between 750–800 cm^{-1} is due to the vibration of the Al—O connection. The band close to 475 cm^{-1} is associated with the vibration of bridged oxygen, based on the deformational vibration of the O—Si—O and Si—O—Al bonds, which in this case, is found in 470 cm^{-1} [11,35–37]. Besides, according to [38], bands of 912 and 539 cm^{-1} are associated with Al—O bonds that suggest the presence of amorphous forms of aluminum oxide and hydroxide (alumina structure), which favors the adsorption of fluoride ions.

Scanning electron microscopy of the calcinated sludge is shown in Fig. 3. The calcinated sludge presents a regular surface and a granular structure of varying sizes, well distributed, with characteristic roughness. The atomic percentages of the EDS analysis in Table 3 indicate the predominance of Fe, Al, Si, and O, components found in the sludge in the form of oxides (SiO_2, $Al2O_3$, and $Fe2O_3$), present due to the use of iron and aluminum-based metallic coagulants in the coagulation-flocculation stage in water treatment plants [32].

Figs. 4 (a) and (b) show the adsorption/desorption isotherm of N_2 and the pore size distribution of the calcinated sludge, respectively. Fig. 4 (a) shows a type IV isotherm, where N_2 adsorption occurs through multiple layers adsorption, followed by capillary condensation. The hysteresis loop between P/P_0 of 0.6–0.9 indicates the predominance of mesopores in the sludge structure [39]. Fig. 4 (b) shows that the largest porous fraction is in the mesoporous region (which comprises the regions from 2 to 50 nm). The results of the BET analysis showed that the surface area of the calcinated sludge was 70.1 $m^2\ g^{-1}$; the average pore size was 11.3 nm, and the average pore volume was 0.12 $m^3\ g^{-1}$.

The point of zero charge (pH_{PZC}) is the pH value of the medium in which the adsorbent material has zero surface charge. In this work, the value obtained for the calcinated sludge was 5.6. Consequently, at pH values below 5.6, the surface of the calcinated sludge is positively charged and, therefore, there is a greater attraction for species with negative charges, such as fluoride [40,41]. Otherwise, at pH greater than 5.6, the surface is negatively charged, resulting in repulsion between the adsorbent particles and the fluoride ions.

Fig. 5 shows the thermogravimetric profile of the calcined sludge. The increase in temperature under an oxidizing atmosphere causes significant changes in the sample mass, which can be identified through the thermogravimetric analysis curve (Fig. 5). The first peak observed at 155 °C is associated with the loss of free or physically bound water to the sludge [27]. Remnants of moisture are still eliminated between 155 and 400 °C, a temperature range that is also attributed to the oxidation of

organic matter present in the sludge. However, a part may still be retained on its surface [42]. This possibly explains the resulting adsorption capacity and the characteristic functional groups identified in infrared spectroscopy, in addition to the slight loss of mass found for temperatures up to 300 °C. The second peak that starts at approximately 375 °C is exothermic and represents the loss of water contained in the aluminum hydroxide and its phase change to γ-Al_2O_3, also called dehydroxylation [26,31]. This process can also occur with clay materials [27,43]. Thus, the material matrix ends up being highly modified for temperatures above 500 °C, which can compromise its fluoride ion adsorption capacity.

It should be considered that the physical and chemical characteristics of the adsorbent plays a major role in the adsorption/removal of fluoride ions. In this case, the characterization techniques show that the that sludge is a complex mixture of several metal oxides, such as aluminum and iron oxides. Besides that, the structure of the calcinated sludge is mainly mesoporous, with a specific surface area of 70 m^2 g^{-1}. The conjunction of these characteristics and the composition of the sludge can improve and directly influence the performance of the adsorbent.

3.2. Optimal conditions for defluorination using calcinated sludge

Defluorination using calcinated sludge was optimized by a central composite rotatable design (CCRD) type (2^2). The optimization was performed in terms of pH and adsorbent dosage. The considered responses were fluoride removal percentage (R, %) and adsorption capacity (q_e, mg g^{-1}). The process was optimized for both a synthetic fluoride solution and a real sample of groundwater collected from a well in Faxinal do Soturno, RS (Brazil). Table 4 shows the matrix used in the experimental design and the respective results of R and q_e, for the adsorption of fluoride ions from groundwater and synthetic solution. Table 4 shows that lower pH values associated with high adsorbent dosages provide greater removals of fluoride ions. However, the adsorption capacity is negatively affected by the increase in adsorbent dosage for both systems.

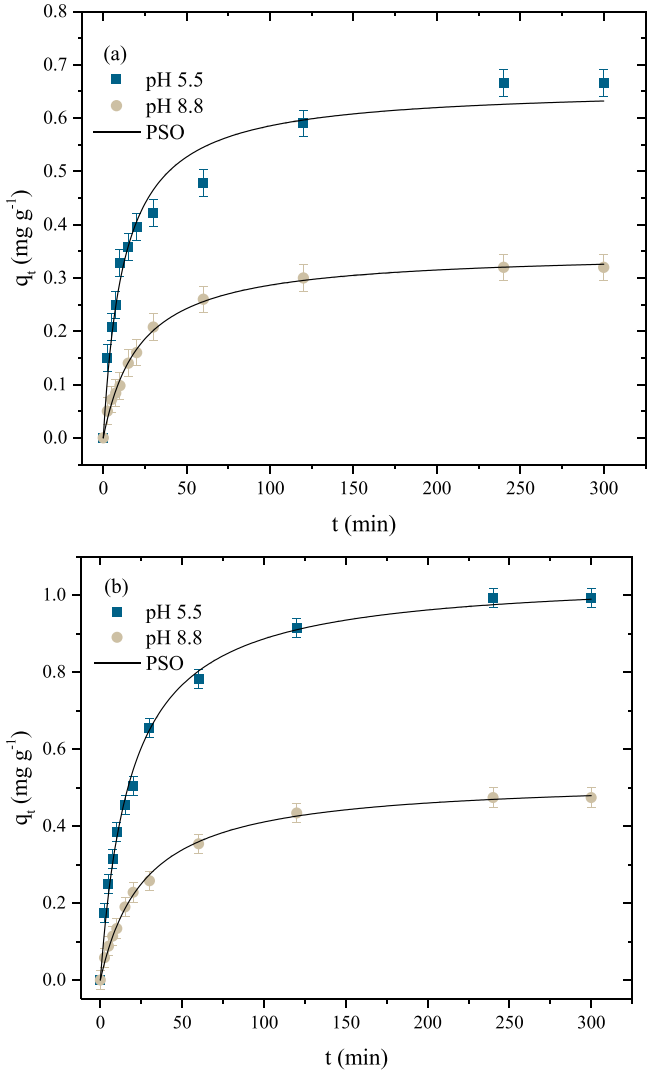

Fig. 9. Adsorption kinetics of fluoride ions from (a) groundwater (b) synthetic solutions.

Pareto graphs for fluoride adsorption from groundwater are shown in Fig. 6 (a) and (b). Pareto graphs for fluoride adsorption from synthetic solutions are depicted in Fig. 6 (c) and (d). From these graphs, it was possible to determine the significant variables for each response, removal (R), and adsorption capacity (q_e). In the graphs, positive values indicate that the independent variables are directly proportional to the response, and negative values show that the independent variables are inversely proportional to the dependent variables.

Taking into account the fluoride adsorption from groundwater, according to Fig. 6 (a), only the interaction between the two variables was not significant in a 95 % confidence interval for the response removal percentage. In Fig. 7 (b), only the quadratic adsorbent dosage variable was not significant within a 95 % confidence interval for the response adsorption capacity. Thus, excluding the non-significant variables, the equations that describe the R and q_e responses as a function of pH and adsorbent dosage are Eq. (1) and Eq. (2):

$$R = 50.07 - 20.89X_1 + 4.11X_1^2 + 12.86X_2 - 4.06X_2^2 \quad (1)$$

$$q_e = 0.71 - 0.34X_1 + 0.10X_1^2 - 0.17X_2 + 0.19X_1X_2 \quad (2)$$

Where X_1 represents the pH, and X_2 represents the adsorbent dosage.

Table 5
Kinetic parameters for fluoride ions adsorption on calcinated sludge.

Kinetic Model	Groundwater		Synthetic solution	
	pH			
	5.5	8.8	5.5	8.8
Pseudo-first-order				
q_1 (mg g^{-1})	0.595	0.3101	0.9408	0.4575
k_1 (min^{-1})	0.0626	0.0381	0.0437	0.0317
R^2	0.9184	0.9891	0.9734	0.9858
R^2_{adj}	0.8086	0.9734	0.9358	0.9655
ARE (%)	14.8789	9.2317	12.5542	11.7748
MSE (mg g^{-1})^2	0.0038	0.0002	0.0032	0.0004
Pseudo-second-order				
q_2 (mg g^{-1})	0.6584	0.3497	1.0502	0.5226
k_2 (g mg^{-1} min^{-1})	0.1220	0.1294	0.0515	0.0702
R^2	0.9732	0.9959	0.9949	0.9975
R^2_{adj}	0.9355	0.9900	0.9875	0.9940
ARE (%)	7.9086	6.2853	5.8069	5.0087
MSE (mg g^{-1})^2	0.0012	0.0001	0.0006	0.0001
General order				
q_n (mg g^{-1})	0.6660	0.3200	0.9920	0.4740
k_n (min^{-1}(g mg^{-1})$^{n-1}$)	0.1590	0.0735	0.0558	0.0541
n (dimensionless)	2.3389	1.4538	1.7472	1.5059
R^2	0.9732	0.9959	0.9949	0.9975
R^2_{adj}	0.9274	0.9888	0.9859	0.9932
ARE (%)	6.5194	6.3799	6.7464	6.6480
MSE (mg g^{-1})^2	0.0011	0.0001	0.0011	0.0002
Avrami				
q_{Av} (mg L^{-1})	0.5950	0.3101	0.9408	0.4575
k_{Av} (min^{-1})	0.1130	0.2171	0.3610	0.2374
n_{Av} (dimensioless)	0.5542	0.1756	0.1211	0.1335
R^2	0.9184	0.9891	0.9734	0.9858
R^2_{adj}	0.7847	0.9701	0.9278	0.9612
ARE (%)	14.8789	9.2317	12.5542	11.7749
MSE (mg L^{-1})^2	0.0038	0.0002	0.0032	0.0004

The determination coefficients (R^2) for Eqs. (1) and (2) were 0.95 and 0.81, respectively, and indicate a satisfactory adjustment of the experimental data to the proposed model.

Considering now the fluoride adsorption from synthetic solutions, for the response R (Fig. 6 (c)), only the interaction between the two variables was not significant, therefore excluding this variable, the model can be given by Eq. (3). For the adsorption capacity response (q_e), according to Fig. 6 (d), all variables were significant so that the model can be given by Eq. (4):

$$R = 67.08 - 11.41X_1 + 3.98X_1^2 + 14.43X_2 - 3.37X_2^2 \quad (3)$$

$$q_e = 1.20 - 0.24X_1 + 0.07X_1^2 - 0.37X_2 - 0.11X_2^2 + 0.13X_1X_2 \quad (4)$$

Where X_1 represents the pH, and X_2 represents the adsorbent dosage.

The determination coefficients (R^2) for Eqs. (3) and (4) were 0.96 and 0.97, respectively, and indicate an optimal adjustment of the experimental data to the proposed model.

Thus, to generate the surface curves that represent R and q_e as a function of pH and adsorbent dosage, the prediction of the models was evaluated using the Fisher test. For groundwater, the value of tabulated F for Eq. (1) was 4.53 while the calculated F was 26.37. For Eq. (2), the tabulated F value was 4.53, while the calculated F was 6.43. For synthetic solutions, the standard F value for Eq. (3) was 4.53, while the calculated F value was 31.01. For Eq. (4), the tabulated F value was 5.05,

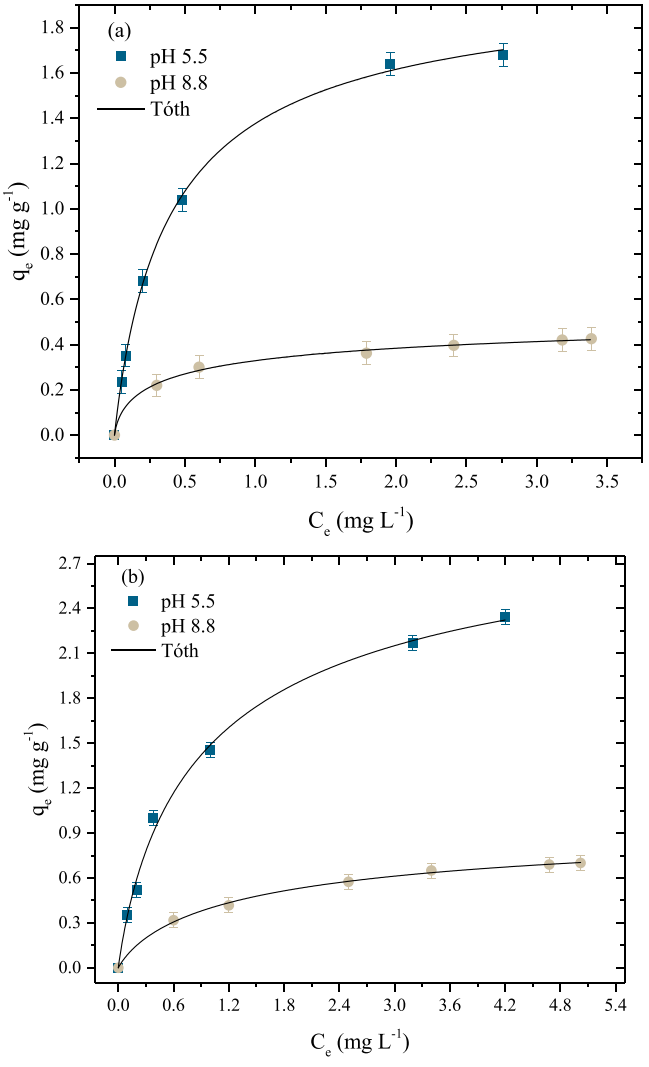

Fig. 10. Adsorption isotherms of fluoride ions from (a) groundwater (b) synthetic solutions.

while the calculated F value was 30.52. Thus, since all calculated F values were greater than the tabulated F values, it is possible to generate the response surfaces, which are presented in Figs. 7 (groundwater) and 8 (synthetic solutions).

Fig. 7 (a) and (b) show the surface curves for fluoride adsorption from groundwater, for the responses R and q_e, respectively. In both figures, a decrease in the pH value leads to greater removal of fluoride ions and greater adsorption capacity. This trend can be explained by the point of zero charge of the calcinated sludge, which is 5.6. In this way, at lower pH values, the sludge surface is positively charged, favoring the electrostatic attraction of negative ions, like fluoride. The adsorption capacity response (q_e) was inversely influenced by the adsorbent dosage, since. However, taking into account the removal percentage, higher adsorbent dosages lead to greater fluoride removals, since a greater number of active adsorptive sites are available. It should be highlighted in the tests with groundwater that a removal above 65 % indicates that the concentration reaches the limit of fluoride ion concentration permitted by the World Health Organization.

Fig. 8 (a) and (b) show the surface curves of the fluoride ion removal (R) and adsorption capacity (q_e) for the experiments using the synthetic solution. Again, both for fluoride ions removal and adsorption capacity, a decrease in the pH value leads to an improvement in the response values, with pHs below 7 already resulting in removals greater than 70 %, ensuring the reach of limits established by World Health Organization. The adsorption capacity was negatively affected by the increase of the adsorbent dosage, having maximum adsorption capacities of 2.07 mg g^{-1} at a pH of 4.9 and an adsorbent dosage of 1.58 g L^{-1}.

Taking into account the recommendation of the World Health Organization, (limit of 1.5 mg L^{-1} of fluoride ions present in potable water), the experiments to determine the kinetics and adsorption isotherms were carried out with the highest adsorbent dosage used in the experimental planning, so that such requirements was met. For the pH, it was observed that lower values lead to greater removals, but the pH

Table 6
Isotherm parameters for fluoride ions adsorption on calcinated sludge.

Isotherm Model	Raw water		synthetic solution	
	pH			
	5.5	8.8	5.5	8.8
Langmuir				
q_L (mg g^{-1})	1.9244	0.4539	2.7150	0.8565
K_L (L mg^{-1})	2.6454	3.0818	1.3075	0.8714
R^2	0.9990	0.9946	0.9956	0.9967
R^2_{adj}	0.9984	0.9920	0.9933	0.9951
ARE (%)	2.9159	2.4227	6.2737	2.8335
MSE (mg g^{-1})^2	0.0006	0.0001	0.0044	0.0003
Freundlich				
K_F ((mg g^{-1})(mg L^{-1})$^{-1/nF}$)	2.2253	0.7876	2.9718	1.0970
$1/n_F$ (dimensionless)	1.6800	0.4260	1.0123	0.4549
R^2	0.9758	0.9951	0.9829	0.9957
R^2_{adj}	0.9637	0.9926	0.9743	0.9935
ARE (%)	18.8470	2.7439	15.8718	2.8242
MSE (mg g^{-1})^2	0.0131	0.0001	0.0169	0.0003
Sips				
q_{mS} (mg g^{-1})	2.2253	0.7876	2.9718	1.0970
K_S (L mg^{-1})	1.6800	0.4260	1.0123	0.4549
n_S (dimensionless)	0.8063	0.4269	0.8745	0.7167
R^2	0.9980	0.9962	0.9965	0.9985
R^2_{adj}	0.9961	0.9925	0.9930	0.9970
ARE (%)	4.6284	2.3341	4.8116	1.6423
MSE (mg g^{-1})^2	0.0013	0.0001	0.0043	0.0001
Tóth				
q_{mT} (mg g^{-1})	2.0380	0.6174	3.1845	1.0500
K_T (L mg^{-1})	2.4791	2.9819	1.3371	1.0911
n_T (dimensionless)	0.8623	0.4589	0.7342	0.6726
R^2	0.9993	0.9967	0.9967	0.9982
R^2_{adj}	0.9986	0.9934	0.9934	0.9964
ARE (%)	1.3623	2.2871	4.6619	1.9207
MSE (mg g^{-1})^2	0.0005	0.0001	0.0040	0.0002

Table 7
Comparison of the maximum adsorption capacity of fluoride ions on various adsorbents.

Adsorbent	Experimental conditions	Experimental conditions	Adsorption capacity (mg g^{-1})
Chelating Resin Containing Phosphonic-Sulfonic Acid Bifunctional Group	pH = 5.2, time =15 h, temperature =303 K, initial concentration =15 mg L^{-1}, adsorbent dose = 2−60 g L^{-1}.	0.63	[44]
Fe(OH)/nano CaO impregnated chitosan composite	pH = 7.1, time =3 h, initial concentration =5 mg L^{-1}, adsorbent dose =8 g L^{-1}.	0.96	[45]
Vatrite calcium carbonate nanoparticles	pH = 5.5, time =2.5 h, temperature =298 K, initial concentration = 10−20 mg L^{-1}, adsorbent dose =5 g L^{-1}.	1.96	[46]
Mechanochemically activated kaolinites	ph = 3, time 1 h, temperature =323 K, initial concentration =20 mg L^{-1}, adsorbent dose =20 g L^{-1}.	0.78	[47]
Clay mixed with hydroxyapatite	pH = 6, time 0.5 h, temperature =305 K, initial concentration = 5−40 mg L^{-1}, adsorbent dose =1.25 g L^{-1}.	18.41	[48]
Bauxite	pH = 6, time 3 h, temperature =303 K, initial concentration = 4−24 mg L^{-1}, adsorbent dose =2 g L^{-1}.	5.16	[49]
Bone char	pH = 7, time 168 h, temperature =298 K, initial concentration = 1−20 mg L^{-1}, adsorbent dose =2 g L^{-1}.	5.89	[50]
Calcium chloride modified natural zeolite	pH = 6, time 6 h, temperature =298 K, initial concentration =100 mg L^{-1}, adsorbent dose =2 g L^{-1}.	1.77	[51]
Eggshell Powder	pH = 6, time 3 h, temperature =303 K, initial concentration = 1.5−20 mg L^{-1}, adsorbent dose =24 g L^{-1}.	1.09	[52]
Graphene Oxide/ Alumina Nanocomposite	pH = 6, time 3 h, temperature =298 K, initial concentration =100 mg L^{-1}, adsorbent dose =4 g L^{-1}.	11.52	[53]
Sweet lemon peel	pH = 4, time 0.67 h, temperature =298 K, initial concentration =20 mg L^{-1}, adsorbent dose =14 g L^{-1}.	1.04	[54]
Banana Peel	pH = 6, time 1 h, temperature =298 K, initial concentration =20 mg L^{-1}, adsorbent dose =16 g L^{-1}.	2.28	[54]
Chitosan	pH = 7, time 3 h, temperature =298 K, initial concentration =5 mg L^{-1}, adsorbent dose =2 g L^{-1}.	1.35	[55]
Calcinated sludge	pH = 5.5, time 4 h, temperature =298 K, initial concentration =5.37 mg L^{-1}, adsorbent dose = 1−15 g L^{-1}.	3.18	This study (synthetic solution)
Calcinated sludge	pH = 5.5, contact time 4 h, temperature =298 K, initial concentration =5.37 mg L^{-1}, adsorbent dose = 1−15 g L^{-1}.	2.04	This study (groundwater)

chosen for performing the kinetics and isotherms was 5.5. This value is lower than the calcinated sludge's point of zero charge (5.6), ensuring that the surface of the material is positively charged, since the surface curves show that good removals were achieved in that pH range. Besides, performing kinetic and isothermal experiments at a pH not as acidic as 4 guarantees a lesser deviation from reality.

3.3. Adsorption kinetics of fluoride ions on calcinated sludge

Kinetics curves were constructed for the fluoride adsorption on calcinated sludge from groundwater and synthetic solutions at different pH values (8.8 and 5.5) (Fig. 9). The pseudo-second-order model was the most adequate to represent the adsorption kinetics of all systems, as shown in Table 5 and Fig. 9. This occurred due to the high values found for the determination coefficient (R^2), adjusted determination coefficient (R^2_{adj}), low values of the relative average error (*ARE*), and *MSE*. The pseudo-second-order kinetic model assumes that that adsorption occurs due to the participation of valence forces or electron exchange between the adsorbate/adsorbent, which is in agreement with the attraction of fluoride ions and adsorbent surface.

The term q_2, which represents the theoretical adsorption capacity of the pseudo-second-order model, was higher when the adsorption experiments occurred at the lower pH. This trend corroborates with the results found for the point of zero charge. The maximum theoretical capacity found for the groundwater sample at pH 5.5 was 0.64 mg g^{-1}, while the synthetic solution, at the same pH, was 1.05 mg g^{-1}. This difference is mainly due to the presence of other ions in the groundwater sample such as chloride, bromide and sulfate (Table 1), which competes with fluoride for the sorption sites. The theoretical values close to the experimental values also indicate an optimal adjustment of the data to the model.

The kinetic curves of both groundwater and synthetic solution tend to a constant adsorption capacity value in a relatively short time of 240 min. For the groundwater sample at a pH of 5.5, a time of just 30 min already causes a 60 % removal in the initial concentration of fluoride

ions, going from 3.6 mg L^{-1} to 1.49 mg L^{-1}, reaching the standards set by the World Health Organization. For a more concentrated synthetic solution, with an initial concentration of 5.37 mg L^{-1}, it takes 60 min to reach the limit stipulated by the World Health Organization. Thus, the calcinated sludge allows, in a short period, to make the water contaminated with fluoride ions drinkable for human consumption and within the WHO standard.

3.4. Adsorption isotherms of fluoride ions on calcinated sludge

Isotherm curves were constructed for the fluoride adsorption on calcinated sludge from groundwater and synthetic solutions at different pH values (8.8 and 5.5). The adsorption isotherm data are shown in Fig. 10 and Table 6. Considering the high values of the determination coefficient (R^2) and the adjusted determination coefficient (R^2_{adj}), and the low values of the average relative error (*ARE*) and *MSE*, the model that best described the adsorption isotherms was the Tóth model. This model is a variation of the Langmuir model, applicable to adsorption on heterogeneous surfaces, where most sites have adsorption energy less than the maximum. The fit of this model is following the heterogeneous characteristics of the calcinated sludge used in this research.

The lower pH values lead to a greater adsorption capacity of the calcinated sludge, where the maximum theoretical capacity found in groundwater was 2.04 mg g^{-1}, whereas, for the synthetic solution, the maximum capacity found was 3.18 mg g^{-1}. At pH 8.8, due to the surface charge presented by the calcinated sludge, lower values of theoretical adsorption capacity were found, of 0.61 mg g^{-1} in groundwater and 1.05 mg g^{-1} in synthetic solution.

Table 7 shows a comparison of several adsorbents for the adsorption of fluoride ions. It is noticed that the calcinated sludge has good adsorption capacity compared to the other adsorbents. Besides, the calcinated sludge used in this work has advantages regarding the other adsorbents, such as simplicity for preparation, ease, abundance, and the cost of obtainment. These findings make the calcinated sludge from water treatment stations a potential adsorbent for the removal of fluoride ions from groundwater.

4. Conclusion

In the present study, it was proposed an eco-friendly and low-cost strategy for groundwater defluorination. Sludge from a water treatment station was modified through calcination and applied as an adsorbent material in the removal of fluoride ions from groundwater. Calcinated sludge presented a semi-crystalline and mesoporous structure, with a specific surface area of 70.1 m^2 g^{-1}, an average pore size of 11.3 nm, and an average pore volume of 0.12 m^3 g^{-1}. The functional groups and other components of the raw sample remained, especially those based on aluminum, iron, and silica, with the elimination of only part of the organic matter due to the calcination process.

The optimal condition for groundwater defluorination was a pH of 5.5 and an adsorbent dosage of 5 g L^{-1}. Under these conditions, the fluoride removal was higher than 70 %; the adsorption capacity was satisfactory and, the WHO limits for fluoride were attained. The kinetic model of pseudo-second-order obtained better adjustment to the experimental data, where times of just 60 min resulted in groundwater with fluoride concentrations below 1.5 mg L^{-1}. For the equilibrium curves, the Tóth model was the one that obtained the best adjustment with the experimental data. The maximum adsorption capacity was 2.04 and 3.18 mg g^{-1} for the groundwater sample and synthetic solution, respectively. It was also observed that the ions present in groundwater, including chloride, bromide, and phosphate, negatively affect the fluoride adsorption capacity. From the results presented, it is possible to consider calcinated sludge from a water treatment station as a potential adsorbent for the removal of fluoride ions from groundwater.

CRediT authorship contribution statement

Renata S. Pigatto: Conceptualization, Investigation, Resources, Writing - original draft. **Dison S.P. Franco:** Methodology, Formal analysis. **Matias S. Netto:** Methodology, Formal analysis. **Élvis Carissimi:** Conceptualization, Writing - review & editing. **Luis F.S. Oliveira:** Conceptualization, Methodology, Formal analysis, Writing - original draft, Visualization. **Sérgio L. Jahn:** Conceptualization, Methodology, Formal analysis, Writing - original draft, Visualization. **Guilherme L. Dotto:** Supervision, Project administration, Funding acquisition, Conceptualization, Writing - review & editing.

Declaration of Competing Interest

The authors report no declarations of interest.

Appendix A. Supplementary data

Supplementary material related to this article can be found, in the online version, at doi:https://doi.org/10.1016/j.jece.2020.104546.

References

[1] S.A. Abo-El-Enein, A. Shebl, S.A. Abo El-Dahab, Drinking water treatment sludge as an efficient adsorbent for heavy metals removal, Appl. Clay Sci. 146 (2017) 343–349, https://doi.org/10.1016/j.clay.2017.06.027.
[2] M. Maraschin, K.F.S.H. Ferrari, A.P.H. da Silva, E. Carissimi, Aluminum sludge thickening: novel helical pipes for aggregation by dual flocculation and thickening by filtration applied to water treatment plants, Sep. Purif. Technol. 241 (2020), https://doi.org/10.1016/j.seppur.2020.116560, 116560.
[3] T.P. Flaten, Aluminium as a risk factor in Alzheimer's disease, with emphasis on drinking water, Brain Res. Bull. 55 (2001) 187–196, https://doi.org/10.1016/S0361-9230(01)00459-2.
[4] E. Siswoyo, I. Qoniah, P. Lestari, J.A. Fajri, R.A. Sani, D.G. Sari, T. Boving, Development of a floating adsorbent for cadmium derived from modified drinking water treatment plant sludge, Environ. Technol. Innov. 14 (2019), https://doi.org/10.1016/j.eti.2019.01.006, 100312.
[5] U. Kumari, S.K. Behera, B.C. Meikap, A novel acid modified alumina adsorbent with enhanced defluoridation property: kinetics, isotherm study and applicability on industrial wastewater, J. Hazard. Mater. 365 (2019) 868–882, https://doi.org/10.1016/j.jhazmat.2018.11.064.
[6] V. Kimambo, P. Bhattacharya, F. Mtalo, J. Mtamba, A. Ahmad, Fluoride occurrence in groundwater systems at global scale and status of defluoridation – state of the art, Groundw. Sustain. Dev. 9 (2019), https://doi.org/10.1016/j.gsd.2019.100223, 100223.
[7] Q. Zhang, S. Bolisetty, Y. Cao, S. Handschin, J. Adamcik, Q. Peng, R. Mezzenga, Selective and efficient removal of fluoride from water: in situ engineered amyloid Fibril/ZrO2 hybrid membranes, Angew. Chemie Int. Ed. 58 (2019) 6012–6016, https://doi.org/10.1002/anie.201901596.
[8] M. Barathi, A.S.K. Kumar, N. Rajesh, Impact of fluoride in potable water – an outlook on the existing defluoridation strategies and the road ahead, Coord. Chem. Rev. 387 (2019) 121–128, https://doi.org/10.1016/j.ccr.2019.02.006.
[9] P. Loganathan, S. Vigneswaran, J. Kandasamy, R. Naidu, Defluoridation of drinking water using adsorption processes, J. Hazard. Mater. 248–249 (2013) 1–19, https://doi.org/10.1016/j.jhazmat.2012.12.043.
[10] M. Mohapatra, S. Anand, B.K. Mishra, D.E. Giles, P. Singh, Review of fluoride removal from drinking water, J. Environ. Manage. 91 (2009) 67–77, https://doi.org/10.1016/j.jenvman.2009.08.015.
[11] K.U. Ahamad, R. Singh, I. Baruah, H. Choudhury, M.R. Sharma, Equilibrium and kinetics modeling of fluoride adsorption onto activated alumina, alum and brick powder, Groundw. Sustain. Dev. 7 (2018) 452–458, https://doi.org/10.1016/j.gsd.2018.06.005.
[12] USEPA, Water Treatment Technology Feasibility Support Document for Chemical Contaminants; In Support of EPA Six-Year Review of National Primary Drinking Water Regulations, Report 815-R-03-004, 2003. http://repositorio.unan.edu.ni/2986/1/5624.pdf.
[13] M.G. Sujana, R.S. Thakur, S.B. Rao, Removal of fluoride from aqueous solution by using alum sludge, J. Colloid Interface Sci. 206 (206) (1998) 94–101, https://doi.org/10.1006/jcis.1998.5611.
[14] S. Brunauer, P.H. Emmett, E. Teller, Adsorption of gases in multimolecular layers, J. Am. Chem. Soc. 60 (1938) 309–319, https://doi.org/10.1021/ja01269a023.
[15] E.P. Barrett, L.G. Joyner, P.P. Halenda, The Determination of Pore Volume and Area Distributions in Porous Substances. I. Computations from Nitrogen Isotherms, J. Am. Chem. Soc. 73 (1951) 373–380, https://doi.org/10.1021/ja01145a126.
[16] D.L. Postai, C.A. Demarchi, F. Zanatta, D.C.C. Melo, C.A. Rodrigues, Adsorption of rhodamine B and methylene blue dyes using waste of seeds of Aleurites moluccana, a low cost adsorbent, Alexandria Eng. J. 55 (2016) 1713–1723, https://doi.org/10.1016/j.aej.2016.03.017.

[17] R.H. Myers, D.C. Montgmoery, C.M. Anderson-Cook, Response Surface Methodology: Process and Product Optimization Using Designed Experiments, third edit, John Wiley & Sons, 2002.
[18] S. Lagergren, About the theory of so-called adsorption of soluble substances, K. Sven. Vetenskapsakademiens Handl. 24 (1898) 1–39.
[19] Y.S. Ho, G. McKay, Kinetic models for the sorption of dye from aqueous solution by wood, Process Saf. Environ. Prot. 76 (1998) 183–191, https://doi.org/10.1205/095758298529326.
[20] A.G. Ritchi, Alternative to the Elovich equation for the kinetics of adsorption of gases on solids BY, J. Chem. Soc. Faraday Trans. 1 Phys. Chem. Condens. Phases 73 (1977) 1650–1653, https://doi.org/10.1039/F19777301650.
[21] M. Avrami, Kinetics of phase change. I: General theory, J. Chem. Phys. 7 (1939) 1103–1112, https://doi.org/10.1063/1.1750380.
[22] I. Langmuir, The adsorption of gases on plane surfaces of glass, mica and platinum, J. Am. Chem. Soc. 40 (1918) 1361–1403, https://doi.org/10.1021/ja02242a004.
[23] H.M.F. Freundlich, Over the adsorption in solution, J. Phys. Chem. 57 (1906) 385–471.
[24] R. Sips, On the structure of a catalyst surface, J. Chem. Phys. 16 (1948) 490–495, https://doi.org/10.1063/1.1746922.
[25] J. Tóth, Calculation of the BET-compatible surface area from any Type I isotherms measured above the critical temperature, J. Colloid Interface Sci. 225 (2000) 378–383, https://doi.org/10.1006/jcis.2000.6723.
[26] S.A. Shahin, M. Mossad, M. Fouad, Evaluation of copper removal efficiency using water treatment sludge, Water Sci. Eng. 12 (2019) 37–44, https://doi.org/10.1016/j.wse.2019.04.001.
[27] Y.P. Ling, R.H. Tham, S.M. Lim, M. Fahim, C.H. Ooi, P. Krishnan, A. Matsumoto, F. Y. Yeoh, Evaluation and reutilization of water sludge from fresh water processing plant as a green clay substituent, Appl. Clay Sci. 143 (2017) 300–306, https://doi.org/10.1016/j.clay.2017.04.007.
[28] M. Muruganandham, S.H. Chen, J.J. Wu, Evaluation of water treatment sludge as a catalyst for aqueous ozone decomposition, Catal. Commun. 8 (2007) 1609–1614, https://doi.org/10.1016/j.catcom.2007.01.018.
[29] G. Schimanke, M. Martin, In situ XRD study of the phase transition of nanocrystalline maghemite (γ-Fe2O3) to hematite (α-Fe2O3), Solid State Ion. 136 (2000) 1235–1240, https://doi.org/10.1016/S0167-2738(00)00593-2.
[30] C. Suksiripattanapong, S. Horpibulsuk, P. Chanprasert, P. Sukmak, A. Arulrajah, Compressive strength development in fly ash geopolymer masonry units manufactured from water treatment sludge, Constr. Build. Mater. 82 (2015) 20–30, https://doi.org/10.1016/j.conbuildmat.2015.02.040.
[31] Á.B. Sifontes, B. Gutierrez, A. Mónaco, A. Yanez, Y. Díaz, F.J. Méndez, L. Llovera, E. Cañizales, J.L. Brito, Preparation of functionalized porous nano-γ-Al2O3 powders employing colophony extract, Biotechnol. Rep. 4 (2014) 21–29, https://doi.org/10.1016/j.btre.2014.07.001.
[32] T. Ahmad, K. Ahmad, A. Ahad, M. Alam, Characterization of water treatment sludge and its reuse as coagulant, J. Environ. Manage. 182 (2016) 606–611, https://doi.org/10.1016/j.jenvman.2016.08.010.
[33] W. Geng, T. Nakajima, H. Takanashi, A. Ohki, Analysis of carboxyl group in coal and coal aromaticity by Fourier transform infrared (FT-IR) spectrometry, Fuel. 88 (2009) 139–144, https://doi.org/10.1016/j.fuel.2008.07.027.
[34] J. Chen, B. Gu, E.J. LeBoeuf, H. Pan, S. Dai, Spectroscopic characterization of the structural and functional properties of natural organic matter fractions, Chemosphere. 48 (2002) 59–68, https://doi.org/10.1016/S0045-6535(02)00041-3.
[35] L. Cormier, D.R. Neuville, G. Calas, Structure and properties of low-silica calcium aluminosilicate glasses, J. Non-Cryst. Solids 274 (2000) 110–114, https://doi.org/10.1016/S0022-3093(00)00209-X.
[36] E.K. Jeon, S. Ryu, S.W. Park, L. Wang, D.C.W. Tsang, K. Baek, Enhanced adsorption of arsenic onto alum sludge modified by calcination, J. Clean. Prod. 176 (2018) 54–62, https://doi.org/10.1016/j.jclepro.2017.12.153.
[37] M.M. Sebdani, J.C. Mauro, L.R. Jensen, M.M. Smedskjaer, Structure-property relations in calcium aluminate glasses containing different divalent cations and SiO2, J. Non Cryst. Solids. 427 (2015) 160–165, https://doi.org/10.1016/j.jnoncrysol.2015.07.047.
[38] S. Goldberg, C.T. Johnston, Mechanisms of arsenic adsorption on amorphous oxides evaluated using macroscopic measurements, vibrational spectroscopy, and surface complexation modeling, J. Colloid Interface Sci. 234 (2001) 204–216, https://doi.org/10.1006/jcis.2000.7295.
[39] C. Sangwichien, G.L. Aranovich, M.D. Donohue, Density functional theory predictions of adsorption isotherms with hysteresis loops, Colloids Surfaces A Physicochem. Eng. Asp. 206 (2002) 313–320, https://doi.org/10.1111/j.1742-7843.2011.00834.x.
[40] M. Gao, W. Wang, H. Yang, B.C. Ye, Efficient removal of fluoride from aqueous solutions using 3D flower-like hierarchical zinc-magnesium-aluminum ternary oxide microspheres, Chem. Eng. J. 380 (2020), https://doi.org/10.1016/j.cej.2019.122459, 122459.
[41] S.S.A. Alkurdi, R.A. Al-Juboori, J. Bundschuh, I. Hamawand, Bone char as a green sorbent for removing health threatening fluoride from drinking water, Environ. Int. 127 (2019) 704–719, https://doi.org/10.1016/j.envint.2019.03.065.
[42] M.A. Tantawy, Characterization and pozzolanic properties of calcined alum sludge, Mater. Res. Bull. 61 (2015) 415–421, https://doi.org/10.1016/j.materresbull.2014.10.042.
[43] J.T. Kloprogge, H.D. Ruan, R.L. Frost, Thermal decomposition of bauxite minerals: infrared emission spectroscopy of gibbsite, boehmite and diaspore, J. Mater. Sci. 37 (2002) 1121–1129, https://doi.org/10.1023/a:1014303119055.
[44] R. Li, X. Tian, I. Ashraf, B. Chen, Fluoride removal using a chelating resin containing phosphonic-sulfonic acid bifunctional group, J. Chromatogr. A 1613 (2020), 460697, https://doi.org/10.1016/j.chroma.2019.460697.
[45] P. Sengupta, S. Saha, S. Banerjee, A. Dey, P. Sarkar, Removal of fluoride ion from drinking water by a new Fe(OH)3/ nano CaO impregnated chitosan composite adsorbent, Polym. Technol. Mater. (2020) 1–13, https://doi.org/10.1080/25740881.2020.1725567.
[46] K.G.M.D. Abeykoon, S.P. Dunuweera, D.N.D. Liyanage, R.M.G. Rajapakse, Removal of fluoride from aqueous solution by porous vatrite calcium carbonate nanoparticles, Mater. Res. Express 7 (2020) 1–21, https://doi.org/10.1088/2053-1591/ab7692.
[47] S. Meenakshi, C.S. Sundaram, R. Sukumar, Enhanced fluoride sorption by mechanochemically activated kaolinites, J. Hazard. Mater. 153 (2008) 164–172, https://doi.org/10.1016/j.jhazmat.2007.08.031.
[48] A.Y. Dang-i, A.O. Boansi, M.M. Pedevoah, Reduction of fluorine in water using clay mixed with hydroxyapatite, Int. J. Appl. Sci. Technol. 5 (2015) 45–55.
[49] M.G. Sujana, S. Anand, Fluoride removal studies from contaminated ground water by using bauxite, Desalination 267 (2011) 222–227, https://doi.org/10.1016/j.desal.2010.09.030.
[50] R. Leyva-Ramos, J. Rivera-Utrilla, N.A. Medellin-Castillo, M. Sanchez-Polo, Kinetic modeling of fluoride adsorption from aqueous solution onto bone char, Chem. Eng. J. 158 (2010) 458–467, https://doi.org/10.1016/j.cej.2010.01.019.
[51] Z. Zhang, Y. Tan, M. Zhong, Defluorination of wastewater by calcium chloride modified natural zeolite, Desalination 276 (2011) 246–252, https://doi.org/10.1016/j.desal.2011.03.057.
[52] R. Bhaumik, N.K. Mondal, B. Das, P. Roy, K.C. Pal, C. Das, A. Banerjee, J.K. Datta, Eggshell powder as an adsorbent for removal of fluoride from aqueous solution: equilibrium, kinetic and thermodynamic studies, J. Chem. 9 (2012) 1457–1480, https://doi.org/10.1155/2012/790401.
[53] N. Xu, S. Li, W. Li, Z. Liu, Removal of fluoride by graphene oxide/alumina nanocomposite: adsorbent preparation, characterization, adsorption performance and mechanisms, ChemistrySelect 5 (2020) 1818–1828, https://doi.org/10.1002/slct.201904867.
[54] A. Mohammad, C.B. Majumder, Removal of fluoride from synthetic waste water by using “Bio-Adsorbents,”, Int. J. Res. Eng. Technol. 03 (2014) 776–785, https://doi.org/10.15623/ijret.2014.0304137.
[55] H. Akbari, S. Jorfi, A.H. Mahvi, M. Yousefi, D. Balarake, Adsorption of fluoride on chitosan in aqueous solutions: determination of adsorption kinetics, Fluoride 51 (2018) 319–327.